NONCONTACT LIFETIME RECONSTRUCTION IN CONTINUOUSLY INHOMOGENEOUS SEMICONDUCTORS: GENERALIZED THEORY AND EXPERIMENTAL PHOTOTHERMAL RESULTS FOR ION-IMPLANTED Si

Alex Salnick and Andreas Mandelis
Photothermal & Optoelectronic Diagnostics Laboratory,
Department of Mechanical and Industrial Engineering, and
Manufacturing Research Corporation of Ontario (MRCO),
University of Toronto, 5 King's College Road,
Toronto, Ontario M5S 3G8,
Canada

Andreas Othonos and Constantinos Christofides
Department of Natural Sciences,
University of Cyprus,
P.O.Box 1678, CY Nicosia,
Cyprus

INTRODUCTION

The common feature of all previous photothermal studies of semiconductors is that only electronically homogeneous materials have been assumed. Correspondingly, both carrier lifetime (τ) and diffusivity (D_n) values have been usually taken to be the bulk characteristics of semiconductor and no experimental works or theoretical models have addressed the problem of τ and D_n depth profile reconstructions. For continuously inhomogeneous solids the treatment of the thermal-wave propagation problem using a Hamilton-Jacobi formalism of the thermal oscillating field has been presented [1] and the concept of the thermal harmonic oscillator (THO) has been successfully used for the thermal diffusivity profile reconstruction [2,3]. The present work is the result of the realization that an electron-hole photoexcited plasma also behaves like a carrier density diffusive wave [4], and, therefore, it can be theoretically treated as a plasma harmonic oscillator (PHO).

THEORETICAL MODEL

In our mathematical treatment we assume a strong optical absorption by a semi-infinite semiconductor having a depth dependent lifetime $\tau(x)$ and diffusivity $D_n(x)$ profile, which extends much deeper than the optical absorption depth. Similar to the thermal-wave case [1] we obtain the PHO Hamiltonian:

$$H(p_n,\alpha)=\frac{1}{2}p_n^2-\frac{i\omega}{2}\alpha^2 \tag{1}$$

which is analog to the classical canonical Hamiltonian function $H(p_n,\alpha)=\frac{1}{2m}p_n^2+\frac{1}{2}K\alpha^2$ with:

$$\alpha=\left[D_n(x)\left(\frac{1+i\omega\tau(x)}{i\omega\tau(x)}\right)\right]^{1/4}N(x) \qquad \text{(position)} \tag{2}$$

$$p_n=D_n(x)\frac{dN(x)}{dx} \qquad \text{(momentum)} \tag{3}$$

Review of Progress in Quantitative Nondestructive Evaluation, Vol 16
Edited by D O. Thompson and D.E Chimenti, Plenum Press, New York, 1997

$$m = 1, \qquad \text{(inertia)} \tag{4}$$

$$K = -\imath\omega \qquad \text{(spring constant)} \tag{5}$$

For the frequency dependence of plasma density $N(x)$ at the surface of electronically inhomogeneous semiconductors it is shown [5] that:

$$N(0,\omega) = N_{0h}(0,\omega)\left[1+\left(R_{n\infty}-1\right)e^{-\left(P_{n\infty}(\omega)-P_{n\infty}(0)\right)}\right] \tag{6}$$

where N_{0h} is the plasma density at the surface of a homogeneous sample,

$$R_{n\infty} \equiv \frac{D_{n0}\sigma_{n0}+s}{D_{n\infty}\sigma_{n\infty}+s} \tag{7}$$

$$P_{n\infty}(\omega) = \lim_{x\to\infty}\left[\sigma_{n\infty}x - H_n(x)\right] \tag{8}$$

$$H_n(x) = \int_0^x \sigma_n(y,\omega)dy \tag{9}$$

where s is the surface recombination velocity, $\sigma_n(x,\omega)$ is the depth dependent plasma wave vector defined as:

$$\sigma_n^2(x,\omega) = \frac{1+\imath\omega\tau(x)}{D_n(x)\tau(x)} \tag{10}$$

and the symbols "0" and "∞" are related to the surface and bulk electronic parameters, respectively. It is shown that for monotonically decreasing or increasing exponential profiles

$$\tau(x) = \tau_\infty\left(1\pm\Delta e^{-qx}\right)^2,\ \Delta = \left|\sqrt{\frac{\tau_0}{\tau_\infty}}-1\right| \quad \text{and} \quad D_n(x) = D_{n\infty}\left(1\pm\delta e^{-qx}\right)^2,\ \delta = \left|\sqrt{\frac{D_{n0}}{D_{n\infty}}}-1\right|, \tag{11}$$

Eqs (6)-(10) yield the exact analytical solution of the forward problem with

$$P_{n\infty}(\omega) = \pm\frac{1}{q}\sqrt{\frac{\imath\omega}{D_{n\infty}}}\left\{\sqrt{1+B^2}\,\ln\left(G_1\right)+(1+\mu)B\ln(G_2)-\sqrt{1+\mu^2B^2}\,\ln\left(G_3\right)\right\} \tag{12}$$

where $B=\left(\imath\omega\tau_\infty\right)^{-1/2}$, $\mu = \delta/(\Delta-\delta)$, $\Delta \neq \delta$, and the logarithmic terms are as follows:

$$G_1 = \frac{1}{2}\left(\frac{|\Delta-1|+B^2}{1+B^2}+\sqrt{\frac{(\Delta-1)^2+B^2}{1+B^2}}\right) \tag{13}$$

$$G_2 = \frac{B+\sqrt{1+B^2}}{B+\sqrt{(\Delta-1)^2+B^2}}|\Delta-1| \tag{14}$$

$$G_3 = \frac{\sqrt{(\Delta-1)^2+B^2}\sqrt{1+\mu^2B^2}+B^2\mu-|\Delta-1|}{\sqrt{1+B^2}\sqrt{1+\mu^2B^2}+B^2\mu-1}|\delta-1|^{-1} \tag{15}$$

In Eqs.(11) and (12) the positive and negative signs are related to decreasing and increasing depth profiles, respectively.

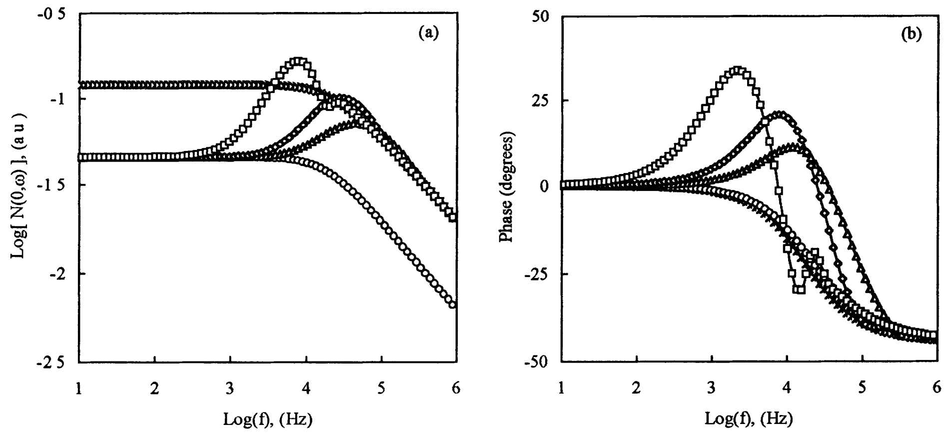

Figure 1. Effect of the steepness constant (q) of the carrier diffusivity profile on the surface plasma density (SPD) magnitude (a) and phase (b) frequency responses for a semiconductor with depth-dependent $D_n(x)$: $q = 10^3$ (□), 5×10^3 (◇) and 10^4 (△) m^{-1}. Parameters used for calculation: D_{n0} = 1 cm^2/s, τ = 10 μs, s = 100 cm/s. Two remaining lines represent a homogeneous sample with D_n = 1 cm^2/s (○) and D_n = 10 cm^2/s (×).

SIMULATIONS OF THE GENERALIZED THEORY

In the following simulations of the carrier dynamics in inhomogeneous semiconductors, increasing electronic diffusivity and/or lifetime profiles will be assumed, corresponding to the physical situation where the semiconductor sample surface is modified (damaged) and the values of the electronic parameters there are lower than those of the unaltered bulk.

The effect of the diffusivity profile steepness constant q is illustrated in Fig.1. At high modulation frequencies, i.e. near the sample surface both the SPD magnitude and phase frequency behavior is that of a homogeneous sample with $D_n = D_{n0}$. Correspondingly, at low frequencies the magnitude and phase are frequency-independent at a level of a homogeneous sample with $D_n = D_{n\infty}$. The steeper the diffusivity profile (higher q), the more confined to the near-surface region the perturbation in the electronic transport properties of the sample, resulting in higher peak probe frequencies for the shallower sub-surface inhomogeneity (Fig 1) Secondary oscillations for the deepest profile ($q = 10^3$ m^{-1}) can also be observed, associated with effective plasma reflections and peak frequency determined by the plasma-wave wavelength becoming commensurate with the thickness of the effective surface layer. Our calculations show that both SPD magnitude and phase are sensitive to the inhomogeneities introduced by spatially varying carrier diffusivity and exhibit a relative signal enhancement with characteristic positive peaks whose amplitudes and positions generally depend on the surface diffusivity value and profile steepness.

In contrast to the variable diffusivity case, inhomogeneities introduced by a spatially varying carrier lifetime result in a clear, sharp negative peak in the SPD magnitude frequency response (Fig.2a) and large phase perturbations (Fig.2b). This negative magnitude peak appears in the frequency range where $\omega\tau \sim 1$, while at low and high modulation frequencies the SPD magnitude dependencies are equivalent to those of a homogeneous sample This feature is a manifestation of the smooth transition of the model to the homogeneous cases with $\tau = \tau_\infty$ and $\tau = \tau_0$ at the respective frequency limits. The amplitude of the inverted peak depends strongly on the gradient of the surface lifetime.

The gradient of the lifetime profile affects the SPD magnitude and phase frequency dependencies nearly in the same manner as with variable diffusivity: a decrease in q shifts the magnitude peak position to lower frequency and makes it more pronounced (Fig.2a). It can be noted that for a changing $\tau(x)$ gradient there is a "critical" profile (indeed, a combination of varying parameters) when the negative peak reaches its maximum value.

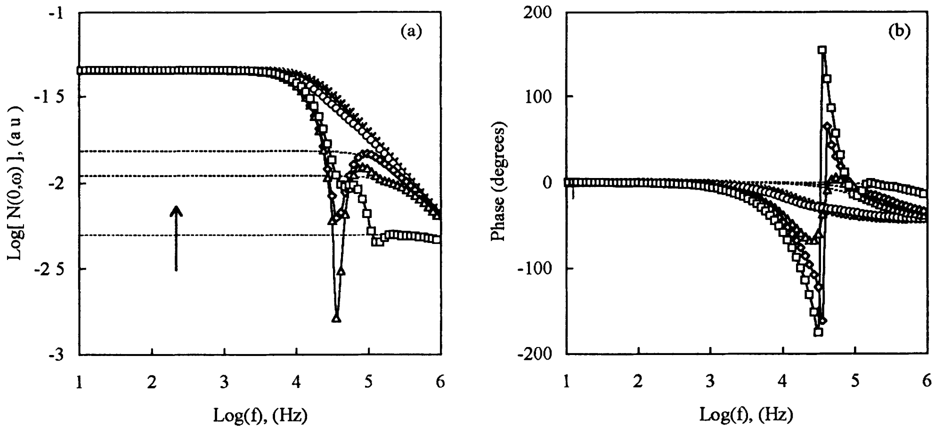

Figure 2. Effect of the surface carrier lifetime (τ_0) on the SPD magnitude (a) and phase (b) frequency responses for a semiconductor with depth-dependent carrier lifetime $\tau(x)$· τ_0 = 0.1 (□), 0.5 (◇), 1.0 (△), 5.0 (○) and 10.0 μs (×). Parameters used for calculation: τ_∞ = 10 μs, D_n = 10 cm²/s, $q = 10^4$ m⁻¹, s = 100 cm/s. The remaining lines in the direction shown in (a) represent a homogeneous sample with τ = 0.1, 0.5 and 1.0 μs, respectively.

Below this value the SPD magnitude frequency behavior becomes more complicated, partly because of plasma-wave reflections across the width of the layer with variable lifetime. The extrema due to plasma reflections appear at higher frequencies with increasing q, i.e. with the narrowing of the inhomogeneous near-surface layer. Overall, both the SPD magnitude and phase are very sensitive to τ_0 and the profile gradient, as described by the q parameter.

In the case of simultaneous depth profiles in carrier diffusivity and lifetime the SPD magnitude and phase frequency responses are a complex superposition of contributions from carrier diffusivity and lifetime inhomogeneities and have a dominant lifetime-like character. It can be shown that only for high frequencies and/or high profile gradient parameter (q) does the combined diffusivity-lifetime term, Eq.(12), become the simple linear superposition of the "pure" diffusivity and lifetime terms, so that both the total magnitude and phase curves can be obtained by an addition of the corresponding dependencies. The effect of D_n and τ spatial gradients in this case is also similar to that for the lifetime profiles. As expected, both magnitude and phase are more sensitive to the lifetime spatial variations than to those of the carrier diffusivity.

THE PLASMA-WAVE INVERSE PROBLEM

The basic feature of plasma-wave depth profiling via consideration of the inverse problem, which makes it quite different from the same procedure in the thermal-wave case [2,3], is that $\tau(x)$ and $D_n(x)$ profiles can be reconstructed only partially.

Due to the peculiar frequency behavior of the a.c. plasma diffusion length $L_n \equiv \sigma_n^{-1}$, Eq.(10), which is frequency-independent when $\omega\tau(x) << 1$ and τ-independent when $\omega\tau(x) >> 1$, for each $\tau(x)$ and/or $D_n(x)$ profile there is a limited depth range within which these profiles can be reconstructed (Fig.3). This range depends on both surface and bulk values, profile steepness and modulation frequency range. As can be seen from Fig.3, even for the homogeneous sample the lifetime profile can be reconstructed within the depth range 12 - 140 μm for the 10 Hz - 1 MHz modulation frequency range used in this example.

Although the expressions derived in the theoretical part of the present work are valid for a monotonically increasing or decreasing carrier diffusivity and lifetime profiles given by Eq.(11), arbitrary $D_n(x)$ or $\tau(x)$ profiles can be handled by redefining (updating) the two constants (q, D_{n0}) or (q, τ_0) at every modulation frequency, starting with the highest frequency, from the experimental data values and assuming knowledge of the values of the carrier transport parameters of the homogeneous reference sample.

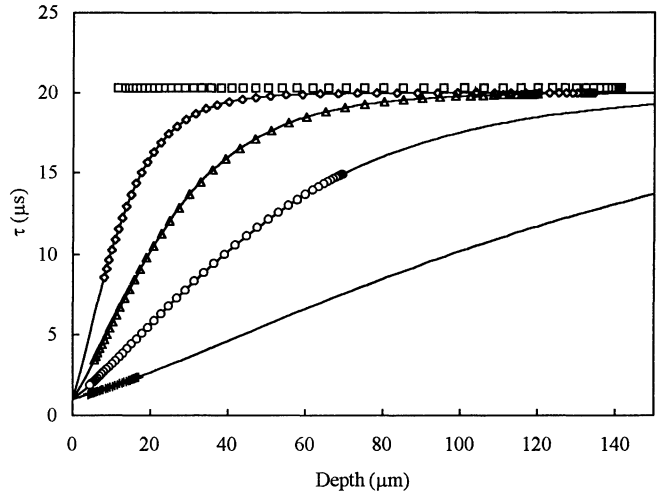

Figure 3. Assumed (lines) and reconstructed (points) made-up carrier lifetime exponential profiles of different steepnesses: homogeneous sample (□), q = 1000 (◇), 500 (△), 250 (○), and 100 cm^{-1} (×). Parameters used: D_n = 10 cm^2/s, τ_0 = 1 μs, τ_∞ = 20 μs, s = 100 cm/s.

Our inversion computer program uses the $M(\omega)$ ratio of the signal for the inhomogeneous sample to that for a reference one and corresponding phases difference $\Phi(\omega)$. The two-dimensional Broyden's method [3] is used for the carrier lifetime depth profile reconstruction which searches for the surface values τ_0 and q satisfying the minimum conditions both in magnitude and phase simultaneously:

$$\left|M_{\exp}(\omega_i)\right| - \left|M_{theor}(\omega_i)\right| = 0 \quad ; \quad \left|\Phi_{\exp}(\omega_i)\right| - \left|\Phi_{theor}(\omega_i)\right| = 0 \tag{16}$$

for each modulation frequency ω_i .

EXPERIMENTAL RESULTS FOR ION-IMPLANTED Si

The experimental setup for the photothermal radiometry (PTR) method [6,7] used to measure the frequency dependencies of the SPD magnitude and phase is shown in Fig.4. A harmonically modulated laser beam obtained by modulating an Ar$^+$ laser using an acousto-optic modulator (AOM) was slightly focused

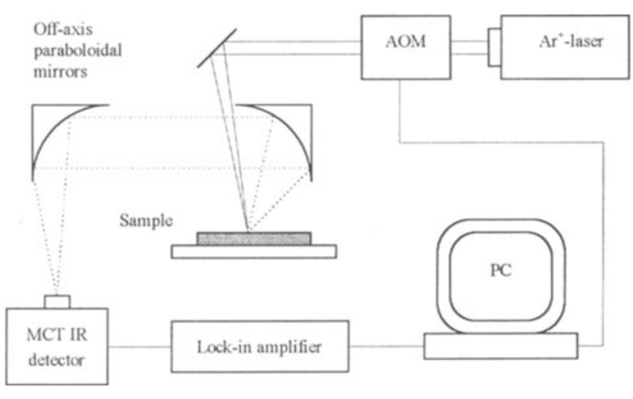

Figure 4 Experimental setup of photothermal infrared radiometry.

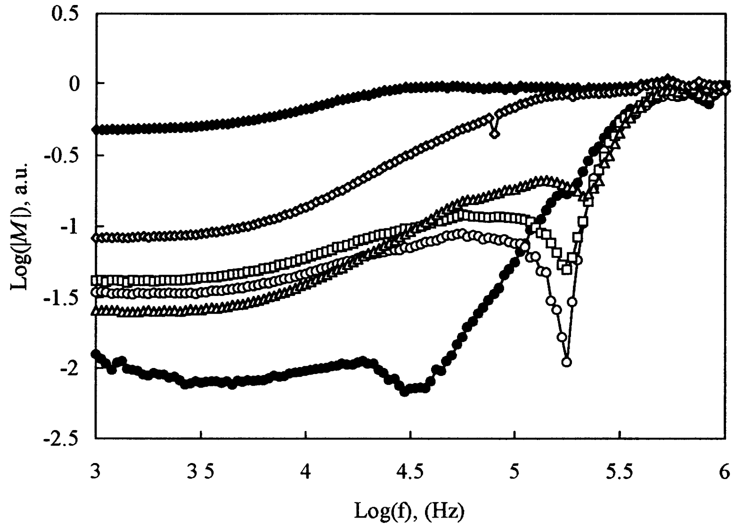

Figure 5. Experimental PTR-amplitude frequency responses obtained for Si samples implanted with P^+ ions (•) and thermally annealed at different temperatures: 350 (○), 500 (□), 800 (♦), 1000 (△) and 1100°C (◇). The curves are normalized to those obtained for non-implanted Si.

on the sample to the size of approximately 3 mm diameter to satisfy the requirements of one-dimensionality. The resulting infra-red radiation emitted from the sample surface was collected by two off-axis paraboloidal mirrors and detected using a liquid N_2-cooled photoconductive mercury-cadmium-telluride (MCT) detector. The PTR signal was then directed to a lock-in amplifier, processed and stored in a personal computer. A set of *n*-type Si samples including one implanted with P^+ ions to the dose of 10^{13} cm^{-2} (50 keV energy) and five implanted and thermally annealed samples at different temperatures was studied. A non-implanted and unannealed Si sample was used as a reference.

Ion-implantation is known to produce a damage in subsurface layers of semiconductors with a peak concentration of implanted ions occurring a few hundreds of angstroms behind the surface. However, the thermally and electronically sensitive defects introduced by ion-implantation are expected to be much deeper than the damaged layer itself. It is also well known that the thermal annealing allows to reconstruct a damaged crystalline structure and reduce the number of both shallow and deep defects in a semiconductor. So, our goal was to study the foregoing electronically-sensitive defects and the process of carrier transport property reconstruction during the thermal anneal by looking at the corresponding carrier lifetime depth profiles.

The PTR frequency-domain method [8] has been used to evaluate the values of carrier diffusivity, carrier lifetime and surface recombination velocity of a non-implanted reference sample. The technique uses simultaneous fitting of both PTR-amplitude and phase experimental frequency responses by a corresponding theoretical model and allows to obtain the foregoing electronic transport parameters in a non-contact and non-destructive manner. For the reference sample used in the present work we obtained $\tau = 75$ μs, $D_n = 20$ cm^2/s and $s = 800$ cm/s.

Figure 5 shows the normalized experimental PTR-amplitude and phase frequency responses obtained for the implanted and annealed Si samples. Although the entire modulation frequency range used was 100 Hz - 1 MHz , for the following inversion analysis the data were taken (and shown in Fig.5) only for the high frequency range of 1 kHz - 1 MHz in order to exclude the contribution from the thermal waves to the total PTR signal which is known to be most significant at low modulation frequencies [9].

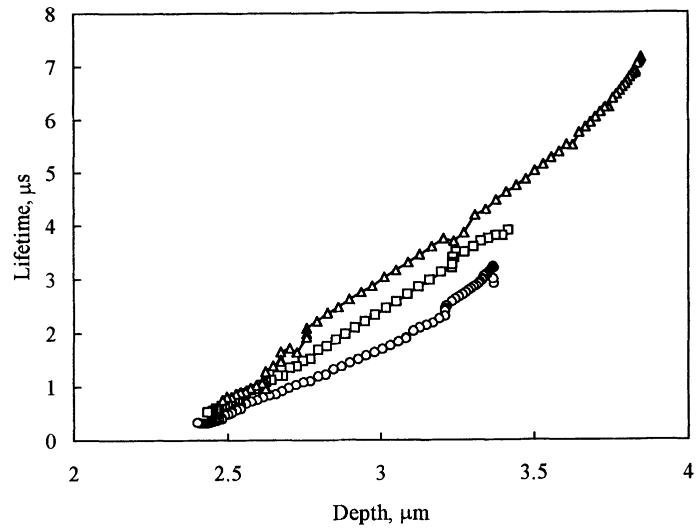

Figure 6. Results of the reconstruction of the carrier lifetime depth profiles from the experimental frequency responses shown in Fig.5: sample annealed at 350 (○), 500 (□), and 1000°C (△).

As can be seen from Fig. 5, the process of ion-implantation introduces a significant change in the PTR-amplitude frequency responses with respect to those of the non-implanted sample. The 350 - 1100°C anneal partially reconstructed the damaged subsurface layers and reduced the number of electronically-sensitive defects in the material bulk as the corresponding amplitude frequency responses are lying closer to those of the reference ($|M(\omega)|$ is close to zero in Fig 5) The most effective restoration of the electronic properties of an implanted sample appeared to be at 800°C The effect of "negative" annealing known from prior photothermal reflectance studies of ion-implanted Si [10] was observed in the present work for the electronic properties as the PTR-amplitude frequency responses for 1000 and 1100°C temperature anneals are close to those obtained after 350-500°C treatments, i.e. in the less effective annealing regimes.

Some of the curves shown in Fig.5, namely those obtained for 350°C and 500°C anneals, exhibit characteristic increasing lifetime behavior with sharp negative amplitude peaks similar to those simulated earlier for exponential $\tau(x)$ profiles (Fig.2). So, for the inversion analysis we assumed spatial variations only in carrier lifetime keeping the value of carrier diffusivity constant and equal to that of the reference sample (20 cm^2/s) Figures 6 and 7 show the results of the carrier lifetime depth profile reconstruction from the experimental PTR-amplitude and phase frequency responses using the inversion algorithm described above. As expected, the ion-implanted unannealed sample with highly damaged subsurface layers has a very short carrier lifetime of about 0.2 µs close to its surface (within 2.5 µm). Annealing treatments at 350°C and 500°C increased the τ values near the surface up to 3 - 4 µs within 3 - 4 µm of depth (Fig. 6). The most effective restoration, from the point of view of the lifetime, appeared to be produced during the thermal annealing at 800°C and resulted in nearly homogeneous carrier lifetime depth profile with much longer τ values of 10-20 µs in the bulk (Fig. 7). However, further increase of annealing temperature to 1000°C doesn't improve electronic property restoration and produces roughly the same result as in the case of low temperature anneals at 350°C and 500°C with τ increasing from 0.5 µs to 7 µs within 4 µm below the sample surface (negative annealing), Fig.6. Finally, the thermal treatment at the highest temperature of 1100°C allows again to improve the electronic properties and brings the bulk carrier lifetime values close to 6 µs (Fig. 7)

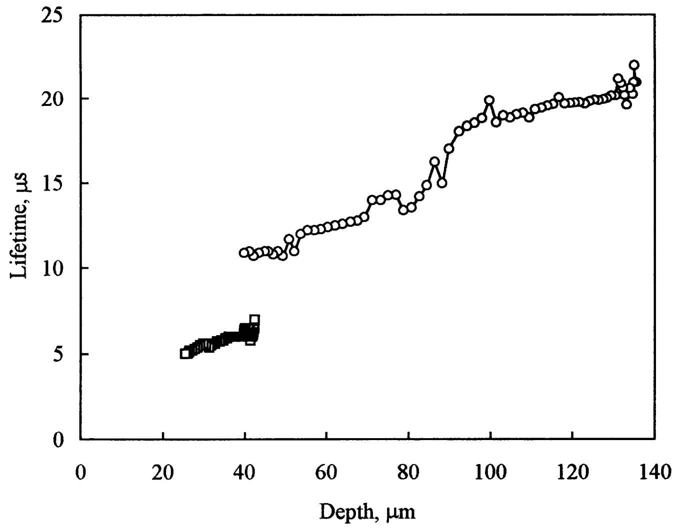

Figure 7. Results of the reconstruction of the carrier lifetime depth profiles from the experimental frequency responses shown in Fig.5: sample annealed at 800 (○) and 1100°C (□).

CONCLUSIONS

The generalized Hamilton-Jacobi plasma-wave theory of a continuously inhomogeneous semiconductor with arbitrary $\tau(x)$ and $D_n(x)$ depth profiles was developed. Carrier plasma-wave amplitude and phase frequency behavior simulations using the developed general theoretical model with specific, physically motivated exponential lifetime and electronic diffusivity depth profiles clearly show the high sensitivity of a frequency scan to spatial changes both in carrier diffusivity and lifetime. These theoretical predictions allow one to distinguish between the dominant contributions from diffusivity and/or lifetime inhomogeneities and evaluate the nature and extent of damage penetration through its effect on the surface and bulk electronic parameters, profile type and steepness. Furthermore, other arbitrary depth profiles can be reconstructed by local matching of the data to an exponential best-fitted profile over a virtual thickness slice determined by the modulation frequency. The general results of the forward path of the depth-profiling problem were further used to address the inverse problem. The first experimental lifetime profile reconstructions were also performed using the two-dimensional Broyden's method for the inverse path on amplitude and phase data from moderately implanted and annealed Si samples probed with infrared photothermal radiometry. Deep electronically-sensitive effects, introduced by ion-implantation and restored by the thermal annealing treatments at different temperatures, were thus observed by reconstructing the corresponding lifetime depth profiles. The effect of the so-called negative annealing on the carrier lifetime was found to produce a decrease in τ values when annealing temperatures are close to 1000°C.

The support of the Natural Sciences and Engineering Research Council of Canada (NSERC) through a Collaborative Project Grant is gratefully acknowledged. One of us (A.S.) ia also grateful to NSERC for a NATO Science Research Fellowship Award.

REFERENCES

1. A. Mandelis, *J. Math. Phys.* 26, 2676 (1985).
2. A. Mandelis, E. Schoubs, S.B.Peralta, and J. Thoen, *J. Appl. Phys.* 70, 1771 (1991).
3. F. Funak, A. Mandelis, and M. Munidasa, *J. de Phys.* III-C7, 4, C7-95 (1994).
4. J. Opsal and A. Rosencwaig, *Appl. Phys. Lett.* 47, 498 (1985).
5 A. Salnick and A. Mandelis, *J. Appl. Phys.* 80 (1996), in press.
6. S. J. Sheard, M. G. Somekh, and T. Hiller, *Mater. Sci. Eng.* B5, 101 (1990).
7. A. Salnick, C. Jean, and A. Mandelis, *Solid-State Electronics* (1996), in press.
8. A. Salnick, A. Mandelis, and C. Jean, *Appl. Phys. Lett.* 69 (1996), in press.
9. A. Mandelis and A. Salnick, to be published.
10. A. Vitkin, C. Christofides, and A. Mandelis, *Appl. Phys. Lett.* 54, 2392 (1989).